Materials Research Proceedings **32** (2023) 220-226 https://doi.org/10.21741/9781644902615-25

Secondary phase precipitation in ultrafine-grained superduplex stainless steels

Alisiya Biserova-Tahchieva[1,a*], Núria Llorca-Isern[1,b] Jose Maria Cabrera[2,c]

[1]Universitat de Barcelona, Departament de Ciència de Materials i Química Física, Martí i Franquès 1-10, E-08028 Barcelona

[2]Universitat Politècnica de Catalunya, Dept. Ciència i Enginyeria de Materials EEBE, c/Eduard Maristany 10-14, E-08019 Barcelona

[a]abiserova.tahchieva@ub.edu, [b]nullorca@ub.edu, [c]jose.maria.cabrera@upc.edu

Keywords: Duplex Stainless Steel, HPT, Severe Plastic Deformation, Secondary Phases

Abstract. Ultrafine-grained S322750 superduplex stainless steel has been obtained through high-pressure torsion (HPT) process. Microstructural evolution after the severe plastic deformation (SPD) has shown no phase transformation. Isothermal heat treatment was applied after the deformation process in order to promote secondary phase precipitation. Precipitation was enhanced in the ultrafine-grained stainless steel in comparison to the coarse-grained stainless steel at the same isothermal heat treatment conditions. Mainly sigma phase and chromium nitrides were found as a product of the local diffusion process. The morphology of the secondary phases has been analyzed by using field emission scanning electron microscopy (FESEM) and transmission electron microscopy (TEM).

Introduction

The increasing global demand for high-performance stainless steels is driven by their significant environmental and economic impact. While renewable energies and alternative energy sources are on the rise, the oil and gas industries still require materials that can withstand geologically challenging reservoir conditions and operational complexities [1]

Duplex stainless steels continue to be utilized in various industries, including chemical engineering, offshore structures, and construction, due to their exceptional properties. These steels exhibit superior toughness, corrosion resistance, and higher strength compared to austenitic stainless steels [2]. Additionally, their cost is lower due to the reduced nickel content. The combination of ferrite (δ) and austenite (γ) phases in equal proportion meets the increased demands for yield strength and corrosion resistance, which cannot be achieved by ferritic or austenitic stainless steels alone.

Furthermore, diverse applications, such as nuclear plant reactors, require careful examination of steel microstructure evolution and the formation of secondary phases. The presence of secondary phases, including sigma (σ) phase, chromium nitrides (CrN, Cr_2N), and carbides ($M_{23}C_6$, M_7C_3), is of significant importance [3]–[6] .Sigma phase is particularly studied for its impact on toughness and corrosion susceptibility due to Cr-depleted zones [7]–[9]. Precipitation of chromium nitrides or carbides, especially in grades with higher nitrogen content, can affect the mechanical properties of the material. Consequently, critical alloying elements such as Cr, Mo, and Ni decompose, leading to a decrease in mechanical and corrosion properties. Extensive research has been conducted on the morphology, size, precipitation mechanism, and orientation relationship between precipitates and the matrix, which are documented in the literature [10]–[13]. However, most of these studies focus on the microstructure of steels immediately after conventional deformation processes or after industrial processing and aging processes, neglecting any previous procedures that may impact microstructural changes. For instance, processing the

Materials Research Proceedings **32** (2023) 220-226 https://doi.org/10.21741/9781644902615-25

steel to achieve an ultrafine-grained microstructure can significantly enhance mechanical properties such as toughness, strength, and fatigue resistance [14]–[16]. Severe plastic deformation (SPD) methods, including high-pressure torsion (HPT), are considered more effective than conventional plastic deformation methods. HPT, a deformation process that minimally affects the dimensions of the object, enables the formation of nanostructures that exhibit substantial improvements in mechanical properties, including superplasticity [17], [18]. It is essential to investigate the combined effects of SPD and thermodynamically induced changes in microstructure.

This study aims to examine the microstructural evolution of UNS S32750 superduplex stainless steel subjected to HPT deformation at room temperature and its impact on the precipitation process. The ultrafine grains and precipitates are analyzed using field-emission scanning electron microscopy (FE-SEM) and transmission electron microscopy (TEM).

Experimental procedure

The material chosen was superduplex stainless steel grade 2507 (UNS S32750), with the following chemical composition: C: 0,018; Si: 0,26; Mn: 0,84; P: 0,019; S: 0,001; Cr: 25,08; Ni: 6,88; Mo: 3,82; N: 0,29; Cu: 0,17, balanced in Fe. For the experiments, disc-shaped samples (10mm diameter and 1mm thick) were prepared by cutting a hot extruded tube. A solution annealing process (1080ºC and held for 30 minutes) was conducted previously, aimed to eliminate any undesirable phases and promote structural homogenization. Subsequently, the samples were quenched in water to rapidly cool them at. The high-pressure torsion (HPT) process was performed at room temperature with an unconstrained setup. The pressure applied during the deformation was 6 GPa. Different numbers of full revolutions, referred to as "turns," were applied: N=1, 5, 10 and 12. The rotation speed of 1 revolution per minute was maintained during the process. The samples were individually placed between a pair of anvils and strained by pressing and rotating the lower anvil. Following the HPT deformation, the samples underwent an isothermal treatment to induce the precipitation of secondary phases (at 830 ±5 ºC for around 3 minutes and rapidly quenched in water). Figure 1 provides a schematic representation of the appearance of the samples, and they were characterized.

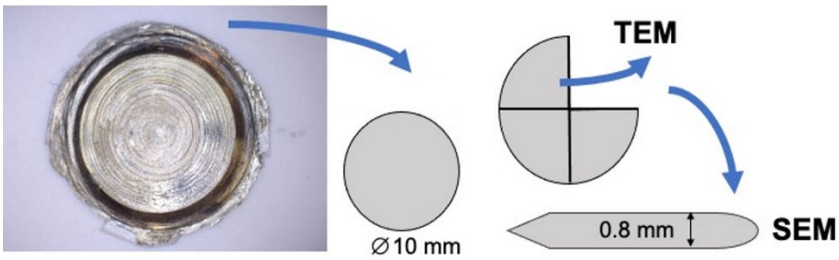

Figure 1. Aspect and dimensions and schematic representation of the characterization of a HPT-deformed sample.

Field-emission scanning electron microscope (FE-SEM) - JEOL J-7100F (JEOL Ltd., Tokyo, Japan) with a coupled Robinson back scattered electron (BSE) detector was used. A JEOL JEM 2100 (JEOL Ltd., Tokyo, Japan) operated at acceleration voltage of 200 kV, equipped with EDS system (80 mm^2 SDD, Oxford Instruments AZtec).

Results and Discussion

Micrographs of the samples deformed by 1, 5, 10 and 12 turns of HPT near the center of the disc samples confirm the deformation of the microstructure. It can be seen the increase of homogeneity from 1 to 12 turns and a similar microstructure with elongated and twisted austenite grains (brighter phase).

Materials Research Proceedings **32** (2023) 220-226 https://doi.org/10.21741/9781644902615-25

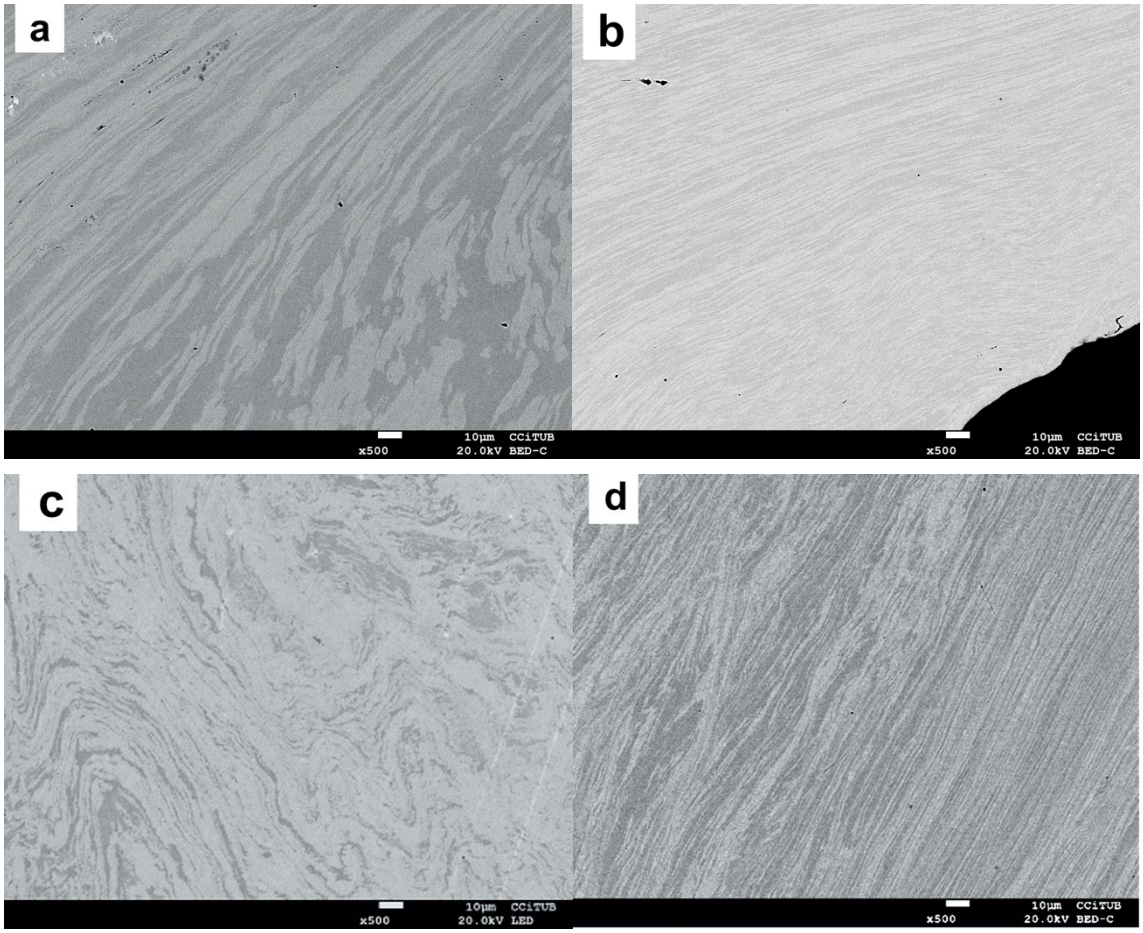

Figure 2. FE-SEM micrographs of SDSS samples near the center of the discs after different number of HPT turns: (a) N=1, (b) N=5, (c) N=10 and (d) N=12.

As observed in Figure 2, there is no evidence of phase transformation or precipitation of secondary phases after HPT. Grains morphology and microstructure analysis has been carried out through TEM.

Bright field (BF) images and selected area diffraction (SAED) patterns have been obtained from the four samples after deformation by 1, 5, 10 and 12 HPT turns. Figure 3 shows the BF micrographs and the SAED patterns, respectively. In Figure 3 (a), the two phases can be seen, in the area highlighted with a dashed yellow line, where the bcc-ferritic phase with less defects is indicated, unlike the fcc-austenite with significant deformation and accumulated dislocations. From the diffraction pattern of the selected zone (marked in Figure 3 (a) with a white circle), the crystallinity of the sample and its random orientation can be appreciated. The fuzzy appearance of grain boundaries is characteristic of non-equilibrium ultrafine grains (UFG) [19]. These, obtained after severe plastic deformation, contain a high density of extrinsic and intrinsic dislocations, as well as elastically distorted layers along the grain boundaries that lead to diffuse images. An example of this aspect can be seen in Figure 3 (b) of the sample after 5 turns. In addition, the accumulation of dislocations forming walls is observed. From the rings of the diffraction patterns, the polycrystallization and the selected zone corresponding to the fcc-ferrite phase are highlighted. As the deformation increases, a greater homogenization is seen, which is reflected in the nanostructure, where after 12 turns, there is a distribution of equiaxed grains and less differentiation between phases, as well as their corresponding diffraction of electrons in the form of diffuse rings, indicating a greater polycrystallization, as can be seen in the image of the

diffraction patterns in Figure 3 (c), highlighting the selected zone corresponding to the fcc-austenite phase.

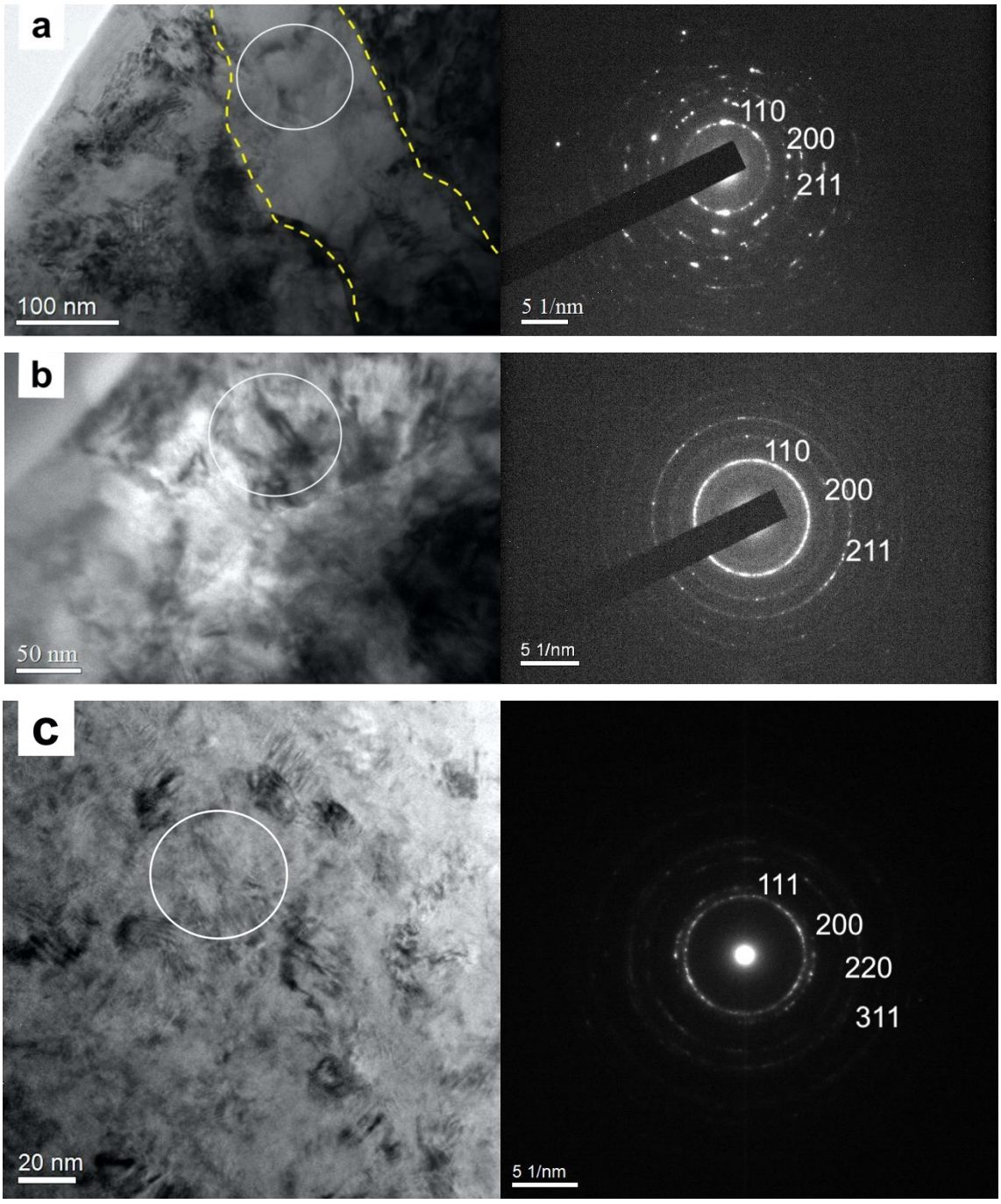

Figure 3. Bright-field TEM micrographs of SDSS deformed samples by HPT: (a) N=1, (b) N=5, (c) N=12 and their corresponding SAED patterns, respectively.

With the short thermal treatment carried out after the HPT process, the precipitation of secondary phases has been easily distinguished in the grains stressed by the deformation, as can be seen in Figure 4. The bright field images of the samples after (a) 1 turn, (b) 5 turns, (c) 10 turns and (d) 12 turns can be observed. The grain size in the different microstructures is relatively comparable, grains between 50 and 100 nm correlated to chromium nitride precipitates and larger grains ~500 nm for the austenite grains and some sigma phase grains. On the other hand, stressed

grains are observed in which the accumulation of dislocations stands out (marked with yellow arrows in Figure 4 (a) and (b). In addition, twinning due to mechanical deformation (marked with red arrows in Figure 4 (a), (b), and (d) can be detected in some grains, characterized by a minimal distortion, sometimes difficult to observe, which can confuse them with twins of thermal origin, but their smaller size, around 100 nm or less, as well as their lenticular shape, are some of the indications to distinguish them from these.

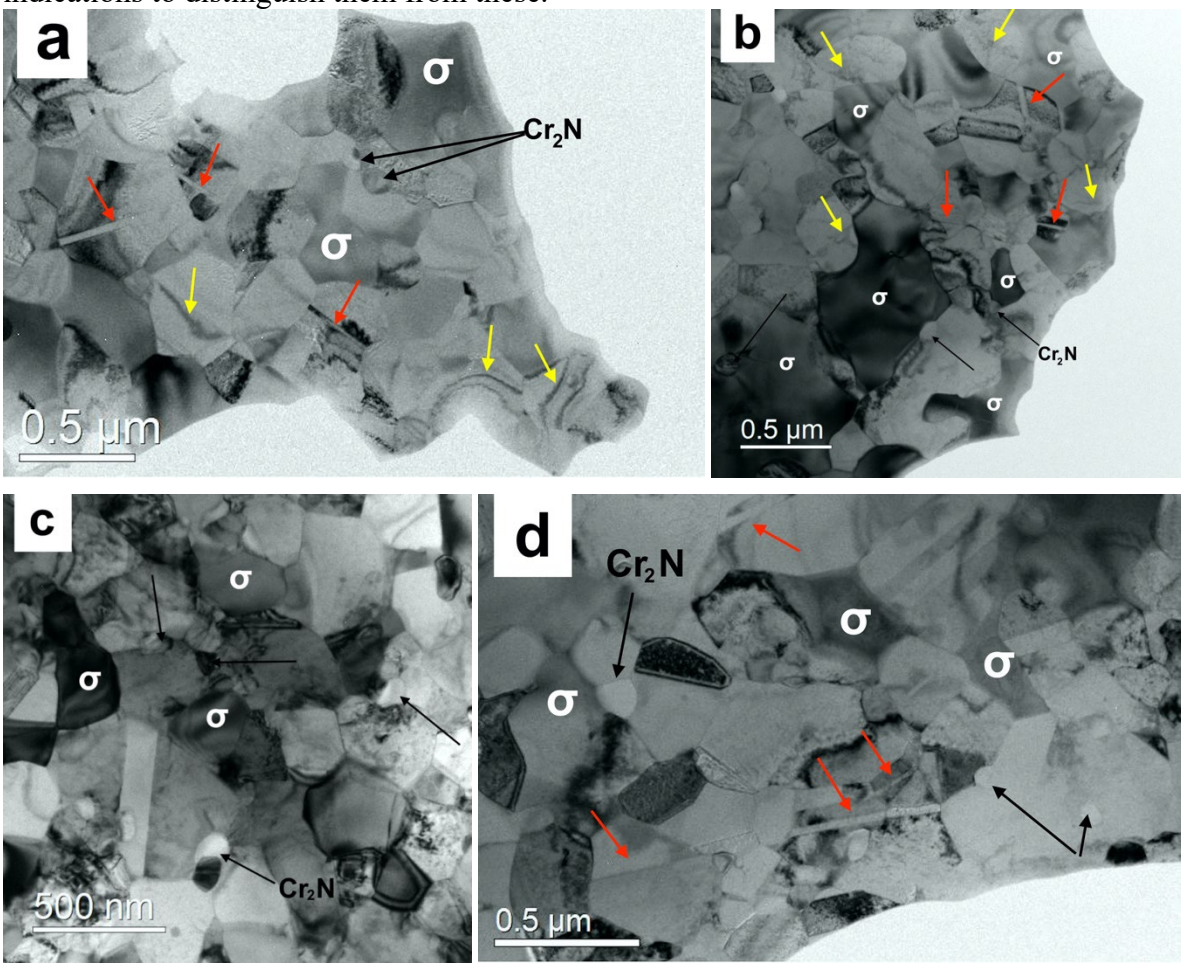

Figure 4. Bright-field TEM micrographs of SDSS deformed samples by HPT and thermally treated: (a) N=1, (b) N=5, (c) N=10 and (d) N=12. Red arrows point out twinning, yellow arrows mark dislocations accumulation and black arrows show some of the Cr_2N.

Smaller grains, around 100 nm, are associated with the precipitates of chromium nitrides (marked with black arrows in Figure 4). The precipitation of Cr_2N has been observed at the grain boundaries of γ/γ, considered as intergranular, as well as in the austenitic grains. The high nitrogen content increases the degree of undercooling, reduces the free energy, and accelerates the precipitation of Cr_2N. The substantial plastic deformation, combined with subsequent temperature exposure, provides favorable conditions for the rapid mobility of nitrogen atoms with a high diffusion coefficient. The precipitation of the sigma phase occurs after the nucleation of the chi phase, as the precipitation temperature of the latter is lower than that of the sigma phase, a phenomenon observed in various studies by multiple authors. Subsequently, the chi phase is gradually consumed by the sigma phase until complete disappearance. In this study, the precipitation of the chi phase was not observed in the severely deformed microstructure after the HPT process. Comparatively with previous studies, secondary phase precipitation was much

greater in the deformed microstructures, and the evolution of the sigma phase was significant enough to completely consume the ferrite phase, as ferrite was not detected.

Due to the continuous diffusion of elements during the precipitation process, starting with the diffusion of nitrogen towards the grain boundaries, the formation of initial intermetallic phases occurs, and chromium nitrides configure zones where some elements decrease while others are in excess. Specifically, after the nucleation of the sigma phase, the diffusion of elements such as Fe, Cr, and Mo from the ferrite phase towards the sigma phase leads to the generation of these depleted zones in Cr and Mo. Moreover, the diffusion of elements from the austenite phase, such as Ni, also results in an enriched zone of Ni. Many authors in literature consider this specific zone generated due to the diffusion of elements and the precipitation of secondary phases as a new phase, referred to as secondary austenite or γ2. It is considered that the precipitation of the sigma phase together with the "secondary austenite" as a eutectoid reaction is not appropriate. Therefore, the same logic applies to the precipitation in superduplex stainless steel, considering it as an invariant transformation.

Conclusions

Superduplex stainless steel has shown no secondary precipitation after HPT deformation. Subsequent isothermal treatment has shown increased precipitation of intermetallic secondary phases. Sigma phase and Cr_2N are the main precipitates found in the microstructure after a short thermal treatment on the 1, 5, 10 and 12 turns of HPT deformed samples. There is a similar trend and homogeneous distribution, as well as size and morphology in the four samples. The sigma phase has precipitated mainly, but not exclusively, at the austenite/chromium nitride/austenite and austenite/austenite/austenite triple point. The results confirmed that chromium nitrides appear to be the preferred nucleation sites for the sigma phase in the most strained samples.

References

[1] B. D. Craig and L. Smith, “Corrosion Resistant Alloys (CRAs) in the oil and gas industry – selection guidelines update,” *Nickel Institute Technical Series*, no. 0073, 2011.

[2] P. Kangas and G. Chai, “Use of advanced austenitic and duplex stainless steels for applications in Oil & Gas and Process industry,” *Century of Stainless Steels*, vol. 794, pp. 645–669, 2013. https://doi.org/10.4028/www.scientific.net/AMR.794.645

[3] L. Pezzato, M. Lago, K. Brunelli, M. Breda, E. Piva, and I. Calliari, “Effect of secondary phases precipitation on corrosion resistance of duplex stainless steels,” in *Materials Science Forum*, Trans Tech Publications Ltd, 2017, pp. 1495–1500. https://doi.org/10.4028/www.scientific.net/MSF.879.1495

[4] G. Argandona, M. V. Biezma, J. M. Berrueta, C. Berlanga, and A. Ruiz, “Detection of Secondary Phases in UNS S32760 Superduplex Stainless Steel by Destructive and Non-destructive Techniques,” *J Mater Eng Perform*, vol. 25, no. 12, pp. 5269–5279, Dec. 2016. https://doi.org/10.1007/s11665-016-2395-7

[5] Y. J. Kim, S. W. Kim, H. B. Kim, C. N. Park, Y. Il Choi, and C. J. Park, “Effects of the precipitation of secondary phases on the erosion-corrosion of 25% Cr duplex stainless steel,” *Corros Sci*, vol. 152, no. March, pp. 202–210, 2019. https://doi.org/10.1016/j.corsci.2019.03.006

[6] K. W. Chan and S. C. Tjong, “Effect of secondary phase precipitation on the corrosion behavior of duplex stainless steels,” *Materials*, vol. 7, no. 7, pp. 5268–5304, 2014. https://doi.org/10.3390/ma7075268

[7] C.-C. Hsieh and W. Wu, “Overview of Intermetallic Sigma () Phase Precipitation in Stainless Steels,” *ISRN Metallurgy*, vol. 2012, pp. 1–16, Mar. 2012. https://doi.org/10.5402/2012/732471

[8] M. B. Cortie and E. M. L. E. M. Jackson, "Simulation of the precipitation of sigma phase in duplex stainless steels," *Metall Mater Trans A Phys Metall Mater Sci*, vol. 28, no. 12, pp. 2477–2484, 1997. https://doi.org/10.1007/s11661-997-0005-x
[9] W. Yongqiang, S. Hao, N. Li, X. Yanhao, and J. Hemin, "Effect of Sigma Phase Precipitation on the Pitting Corrosion Mechanism of Duplex Stainless Steels," *Int. J. Electrochem. Sci*, vol. 13, pp. 9868–9887, 2018. https://doi.org/10.20964/2018.10.38
[10] A. D. Warren, R. L. Harniman, Z. Guo, C. M. Younes, P. E. J. Flewitt, and T. B. Scott, "Quantification of sigma-phase evolution in thermally aged 2205 duplex stainless steel," *J Mater Sci*, vol. 51, no. 2, pp. 694–707, Jan. 2016. https://doi.org/10.1007/s10853-015-9131-9
[11] N. Llorca-Isern, H. López-Luque, I. López-Jiménez, and M. V. Biezma, "Identification of sigma and chi phases in duplex stainless steels," *Mater Charact*, vol. 112, pp. 20–29, Feb. 2016. https://doi.org/10.1016/j.matchar.2015.12.004
[12] J. S. Li *et al.*, "Thermal cycling induced stress–assisted sigma phase formation in super duplex stainless steel," *Mater Des*, vol. 182, 2019. https://doi.org/10.1016/j.matdes.2019.108003
[13] R. O. Sousa, P. Lacerda, P. J. Ferreira, and L. M. M. Ribeiro, "On the Precipitation of Sigma and Chi Phases in a Cast Super Duplex Stainless Steel," *Metallurgical and Materials Transactions A*, vol. 50, no. 10, pp. 4758–4778, 2019. https://doi.org/10.1007/s11661-019-05396-6
[14] R. Z. Valiev, Y. Estrin, Z. Horita, T. G. Langdon, M. J. Zehetbauer, and Y. Zhu, "Producing Bulk Ultrafine-Grained Materials by Severe Plastic Deformation: Ten Years Later," *JOM*, vol. 68, no. 4, pp. 1216–1226, Apr. 2016. https://doi.org/10.1007/s11837-016-1820-6
[15] M. Kawasaki, H.-J. Lee, B. Ahn, A. P. Zhilyaev, and T. G. Langdon, "Evolution of hardness in ultrafine-grained metals processed by high-pressure torsion," *Journal of Materials Research and Technology*, vol. 3, no. 4, pp. 311–318, Oct. 2014. https://doi.org/10.1016/J.JMRT.2014.06.002
[16] T. G. Langdon, "Twenty-five years of ultrafine-grained materials: Achieving exceptional properties through grain refinement," *Acta Mater*, vol. 61, no. 19, pp. 7035–7059, Nov. 2013. https://doi.org/10.1016/j.actamat.2013.08.018
[17] A. P. Zhilyaev and T. G. Langdon, "Using high-pressure torsion for metal processing: Fundamentals and applications," *Prog Mater Sci*, vol. 53, no. 6, pp. 893–979, Aug. 2008. https://doi.org/10.1016/j.pmatsci.2008.03.002
[18] K. Edalati and Z. Horita, "A review on high-pressure torsion (HPT) from 1935 to 1988," *Materials Science and Engineering: A*, vol. 652, pp. 325–352, Jan. 2016. https://doi.org/10.1016/j.msea.2015.11.074
[19] R. Z. Valiev, V. Yu. Gertsman, and O. A. Kaibyshev, "Grain boundary structure and properties under external influences," *physica status solidi (a)*, vol. 97, no. 1. John Wiley & Sons, Ltd, pp. 11–56, Sep. 16, 1986. doi: 10.1002/pssa.2210970102